

A Multidataset Assessment of Climatic Drivers and Uncertainties of Recent Trends in Evaporative Demand across the Continental United States

CHRISTINE M. ALBANO,^a JOHN T. ABATZOGLOU,^b DANIEL J. MCEVOY,^c JUSTIN L. HUNTINGTON,^a
CHARLES G. MORTON,^d MICHAEL D. DETTINGER,^e AND THOMAS J. OTT^a

^a *Division of Hydrologic Sciences, Desert Research Institute, Reno, Nevada*

^b *Management of Complex Systems Department, University of California, Merced, Merced, California*

^c *Division of Atmospheric Sciences, Desert Research Institute, Reno, Nevada*

^d *Division of Earth and Ecosystem Sciences, Desert Research Institute, Reno, Nevada*

^e *California–Nevada Climate Applications Program, Scripps Institution of Oceanography, La Jolla, California*

(Manuscript received 24 August 2021, in final form 7 January 2022)


ABSTRACT: Increased atmospheric evaporative demand has important implications for humans and ecosystems in water-scarce lands. While temperature plays a significant role in driving evaporative demand and its trend, other climate variables are also influential and their contributions to recent trends in evaporative demand are unknown. We address this gap with an assessment of recent (1980–2020) trends in annual reference evapotranspiration (ET_o) and its drivers across the continental United States based on five gridded datasets. In doing so, we characterize the structural uncertainty of ET_o trends and decompose the relative influences of temperature, wind speed, solar radiation, and humidity. Results highlight large and robust changes in ET_o across much of the western United States, centered on the Rio Grande region where ET_o increased 135–235 mm during 1980–2020. The largest uncertainties in ET_o trends are in the central and eastern United States and surrounding the Upper Colorado River. Trend decomposition highlights the strong and widespread influence of temperature, which contributes to 57% of observed ET_o trends, on average. ET_o increases are mitigated by increases in specific humidity in non-water-limited regions, while small decreases in specific humidity and increases in wind speed and solar radiation magnify ET_o increases across the West. Our results show increases in ET_o across the West that are already emerging outside the range of variability observed 20–40 years ago. Our results suggest that twenty-first-century land and water managers need to plan for an already increasing influence of evaporative demand on water availability and wildfire risks.


SIGNIFICANCE STATEMENT: Increased atmospheric thirst due to climate warming has the potential to decrease water availability and increase wildfire risks in water-scarce regions. Here, we identified how much atmospheric thirst has changed across the continental United States over the past 40 years, what climate variables are driving the change, and how consistent these changes are among five data sources. We found that atmospheric thirst is consistently emerging outside the range experienced in the late twentieth century in some western regions with 57% of the change driven by temperature. Importantly, we demonstrate that increased atmospheric thirst has already become a persistent forcing of western landscapes and water supplies toward drought and will be an essential consideration for land and water management planning going forward.

KEYWORDS: North America; Climate change; Evapotranspiration; Trends

1. Introduction

The capacity of Earth's atmosphere to hold water vapor is increasing nonlinearly with rising global temperatures. This has important implications in terms of intensification of the hydrologic cycle and the land surface energy budget (Huntington 2006), as well as greenhouse gas concentrations, given

 Denotes content that is immediately available upon publication as open access.

 Supplemental information related to this paper is available at the Journals Online website: <https://doi.org/10.1175/JHM-D-21-0163.s1>.

Corresponding author: Christine Albano, christine.albano@dri.edu

that water vapor is, itself, a greenhouse gas (Brown and Degaetano 2013). Atmospheric evaporative demand is defined as the maximum amount of evapotranspiration that would occur, given atmospheric conditions and an unlimited supply of surface moisture (Hobbins and Huntington 2016). In water-limited regions such as the western United States, anomalously high atmospheric evaporative demand over seasonal and annual time scales is strongly associated with drought (Hobbins et al. 2016; McEvoy et al. 2016), increased plant-water stress (Grossiord et al. 2020; Williams et al. 2013), increased forest fire area (Abatzoglou and Kolden 2013; Abatzoglou and Williams 2016), and reduced streamflow (Udall and Overpeck 2017; Das et al. 2011). In non-water-limited regions, increased evaporative demand may result in increased plant water use, which in turn can serve to partially or fully acquiesce and suppress atmospheric demand by increasing the amount of water vapor in the air, but may

DOI: 10.1175/JHM-D-21-0163.1

© 2022 American Meteorological Society. For information regarding reuse of this content and general copyright information, consult the [AMS Copyright Policy](#) (www.ametsoc.org/PUBSReuseLicenses).

come at the cost of reductions in streamflow (Kramer et al. 2015) and depletion of shallow groundwater (Condon et al. 2020).

In the western United States, the impacts of warming climate and drought conditions in the twenty-first century are well documented, including extended fire seasons with more large fires (Dennison et al. 2014) and increasing area burned (Westerling et al. 2006), dwindling water supplies (Udall and Overpeck 2017), and widespread tree mortality (Fettig et al. 2019; Williams et al. 2013). While precipitation variability has historically been the dominant driver of drought conditions (Ficklin et al. 2015), research has highlighted the substantial role of increased temperature (Mote et al. 2016; Diffenbaugh et al. 2015; Woodhouse et al. 2016) and evaporative demand (Williams et al. 2020; Abatzoglou and Williams 2016) on drought conditions in recent years. Yet, despite increasing attention to this demand side of drought, a systematic quantification of evaporative demand change, what climate variables are predominantly driving this change, and how robust changes are across different datasets is lacking.

Although temperature plays a dominant role in influencing atmospheric evaporative demand, other variables also contribute to this demand including the amount of atmospheric water vapor, wind-driven movement of heat and water away from the land surface, and the amount of radiative energy available at the land surface to convert water from liquid to vapor (Monteith 1965). These other variables vary in their influence among seasons, locations, and time scales and can be important drivers of variability (Hobbins 2016) and trends (Ficklin et al. 2015) in evaporative demand in some instances. Thus, it is important to understand how all of these variables have changed over time, and how these changes relate to variations in evaporative demand.

Multiple studies have assessed recent trends in aridity and atmospheric evaporative demand across the conterminous United States (CONUS) and globally. These studies have generally pointed to differences in the direction of trends across gradients of water availability, with increases in evaporative demand (Sheffield et al. 2012; McCabe and Wolock 2015; Ficklin et al. 2015; Vicente-Serrano et al. 2020) and expansion of arid lands (Feng and Fu 2013) across much of the arid western and southwestern United States and decreases in evaporative demand in some parts of the eastern United States (McCabe and Wolock 2015; Sheffield et al. 2012; Ficklin et al. 2015), where increases in precipitation (Ficklin et al. 2015; Bishop et al. 2021) and soil moisture (Groisman et al. 2004; Andreadis and Lettenmaier 2006) have been observed.

Although studies have found general agreement of trends in evaporative demand across the CONUS, most studies have typically been based on one set of forcing conditions (Ficklin et al. 2016, 2015; McCabe and Wolock 2015; Vicente-Serrano et al. 2020) or a limited number of ground observations (Groisman et al. 2004; Lawrimore and Peterson 2000; Hobbins et al. 2004; Szilagyi et al. 2001). Likewise, other studies have focused on trends in actual evapotranspiration (ETa; Walter et al. 2004; Jasinski et al. 2019)—the flux of water transferred from the land surface to the atmosphere,

rather than evaporative demand. And while several studies have been conducted to assess trends in individual variables that contribute to evaporative demand including temperature (Vose et al. 2012), wind (Vautard et al. 2010; Pryor et al. 2009; Zhang et al. 2019; Fan et al. 2021), solar radiation (Augustine et al. 2019), and humidity (Ficklin and Novick 2017; Brown and Degaetano 2013; Alter et al. 2018; Seager et al. 2015), differences in analytical approaches, datasets, and time periods analyzed make it difficult to ascertain how these may collectively influence changes in evaporative demand. Moreover, many of these studies have identified biases and lack of agreement among datasets (e.g., Slater 2016; Fan et al. 2021; Boilley and Wald 2015) that suggest the potential for substantial uncertainties in resultant trends in evaporative demand. In this study, we seek to address these gaps by conducting a systematic and spatially explicit assessment of trends in both evaporative demand and its component drivers at seasonal and annual time scales, across the CONUS, and across multiple data sources. In doing so, we leverage an ensemble of reanalysis and gridded climate products and the Google Earth Engine cloud computing environment (Gorelick et al. 2017) to address three primary research questions, including 1) how do trends in evaporative demand vary across the CONUS, 2) what climate variables are most responsible for evaporative demand trends, and 3) how consistent and significant are trends across an ensemble of reanalysis and gridded climate products?

2. Methods

Reference evapotranspiration (ET_o), as estimated using the Penman–Monteith equation and standardized by the American Society of Civil Engineers (ASCE; Allen et al. 2005), provides a useful and consistent measure of evaporative demand by assuming an idealized and specific well-watered “reference” surface (Hobbins and Huntington 2016). ET_o represents a standardized form of potential evapotranspiration, whereby the surface conditions for a reference crop, including crop height, surface resistance to water vapor flow, and albedo are specified. This standardization is useful for climatological studies as it enables atmospheric drivers of evaporative demand to be isolated from drivers associated with surface conditions, which may be more difficult to measure and can vary substantially among locations. The ASCE standardized form of daily ET_o (mm) for a short (0.12-m height) grass reference crop with a surface resistance (driven by stomatal conductance, leaf area, and soil surface) of 70 s m⁻¹, and albedo equal to 0.23 is defined as

$$ET_o = \frac{0.408\Delta(R_n - G) + \gamma \frac{C_n}{T + 273} u_2 (e_s - e_a)}{\Delta + \gamma(1 + C_d u_2)}, \quad (1)$$

where Δ = the slope of the saturation vapor pressure–temperature curve (kPa °C⁻¹), R_n = calculated net radiation at the grass surface (MJ m⁻² day⁻¹), G = soil heat flux density at the soil surface (MJ m⁻² day⁻¹), γ = the psychrometric constant (kPa °C⁻¹), C_n = 900 K mm s³ Mg⁻¹ day⁻¹ for a short grass

reference, T = mean daily temperature at 2-m height ($^{\circ}\text{C}$), u_2 = mean daily wind speed at 2-m height in (m s^{-1}), e_s = mean daily saturation vapor pressure at 2-m height, calculated from daily minimum and maximum temperatures (kPa), e_a = mean actual vapor pressure at 2-m height, calculated from e_s and specific humidity (kPa), and $C_d = 0.34 \text{ m s}^{-1}$ for a short grass reference. In this equation, the difference between e_s and e_a represents the vapor pressure deficit (VPD), which is the difference between the amount of water vapor the atmosphere can hold and actual water vapor content. VPD is an important driver of evaporative demand (Ficklin and Novick 2017).

Unlike other estimators of evaporative demand that use only empirical relations with temperature under current climatic conditions as their basis, Penman–Monteith ETo is physically based and incorporates measures of solar radiation, temperature, humidity, and wind speed to account for both the radiative and advective components of evaporative demand (Monteith 1965; Allen et al. 1998). As such, the use of ETo, rather than estimators based on temperature alone, provides better representation of past and future changes in evaporative demand because it accounts for the multiple drivers of ETo that may all be changing over time or may differ in their relative importance over space (Hobbins et al. 2017; Sheffield et al. 2012; Vicente-Serrano et al. 2020). The trade-off is that solar radiation, wind speed, and humidity data may not be as readily available as temperature data (Vicente-Serrano et al. 2020) and uncertainties in these data sources can ultimately affect ETo calculations and should be accounted for when possible (McAfee 2013; Fisher et al. 2011). In addition, surface resistance is set to a fixed (i.e., standardized) value for the calculation of Penman–Monteith ETo and therefore does not account for differences over space (e.g., due to differences in plant species; Fisher et al. 2011) or time (e.g., due to decreased plant stomatal conductance on the basis of increased CO_2 concentrations), the latter of which may result in overestimation of future ETo relative to radiation-only based methods (Milly and Dunne 2016, 2017). While parameterizing ETo calculations to address differences over space is outside the scope of this study, which is focused on the climatological drivers of evaporative demand, we did confirm that the effects of changing CO_2 concentrations over the 41-yr period examined in our study (following methods in Yang et al. 2019) were minimal and therefore did not significantly affect our results (supplemental information S11).

a. Datasets

We assessed trends in ETo and its drivers using five datasets, including the European Centre for Medium-Range Weather Forecasts Reanalysis (ERA5; Hersbach et al. 2018, 2020), GridMET (Abatzoglou 2013), the Japanese 55-year reanalysis (JRA-55; Kobayashi et al. 2015; Japan Meteorological Agency 2013), the Modern-Era Retrospective Analysis for Research and Applications, version 2 (MERRA-2; Gelaro et al. 2017; Global Modeling and Assimilation Office

2015), and the North American Land Data Assimilation System (NLDAS-2; Xia et al. 2012, 2009). While these datasets differ considerably in their spatial resolutions, source observations, and temporal extents they were selected for analysis over other readily available datasets because of these differences, and because they all include the variables needed (i.e., minimum and maximum daily temperature, wind speed, incoming solar radiation, and humidity) to calculate the ASCE standardized Penman–Monteith equation (Allen et al. 2005).

Global reanalysis datasets, including ERA5, MERRA-2, and JRA-55 are relatively coarse in spatial scale, ranging from approximately 30–55-km spatial resolution across CONUS with hourly to 6-hourly temporal resolution. Some observational datasets are common to multiple reanalyses; for example, the observational dataset used in JRA-55 is the same as ERA-40, a previous iteration of ERA5, and all three of these datasets draw from common conventional and satellite datasets (see McCarty et al. 2016; Kobayashi et al. 2015; <https://confluence.ecmwf.int/display/CKB/ERA5%3A+data+documentation#ERA5:datadocumentation-Observations>). These commonalities thereby limit reanalyses from being truly independent although the assimilation algorithms and data combinations differ considerably. For each of these datasets, the number of observations assimilated has increased substantially over the course of the study period (Hersbach et al. 2020; Gelaro et al. 2017; Kobayashi et al. 2015) and the technologies used for measurement have evolved (Fan et al. 2021); such changes have the potential to affect trends over time (Wen et al. 2019).

NLDAS-2 is a ~12.5-km resolution hourly land surface model that inherits forcing data primarily from the ~32-km resolution North American Regional Reanalysis (NARR; Mesinger et al. 2006), which is, itself, a high-resolution extension of the NCEP–NCAR global reanalysis. The finer resolution of NLDAS-2 is achieved by spatially interpolating and temporally disaggregating temperature, humidity and wind data from NARR. Downward surface shortwave radiation from NARR is bias corrected using observations (Cosgrove et al. 2003). The daily resolution GridMET dataset is a hybrid of NLDAS-2 and the Parameter-Elevation Regressions on Independent Slopes Model (PRISM; Daly et al. 2008). GridMET integrates the high spatial resolution interpolation of humidity, temperature, and precipitation observations from PRISM, and temporally disaggregates these based on NLDAS-2 to take advantage of its high temporal resolution. Incoming solar radiation and wind speeds are inherited directly from NLDAS-2.

We calculated daily ETo for each grid cell of each dataset at its native resolution using the ASCE Standardized ETo equation for a grass reference surface (Allen et al. 2005). For each dataset, we created daily summaries of minimum and maximum temperature, average wind speed, average specific humidity, and total incoming solar radiation. After calculating daily ETo, we aggregated ETo and its input variables to the annual scale for trend assessments.

b. Trend assessment

We assessed spatially explicit trends in annual ETo for each grid cell and dataset for the 1980–2020 time period based on the nonparametric Theil–Sen slope estimator, which tends to be robust to outliers (Sen 1968), using the Google Earth Engine cloud computing platform (Gorelick et al. 2017). While maps for individual datasets were calculated and visualized at their native spatial resolution, data were resampled to a common 12-km resolution prior to calculating among-dataset means and standard deviations. In addition to the spatially explicit trend assessment, we spatially averaged annual ETo over 18 USGS hydrologic unit code (HUC-2) water resource regions (Fig. 1), which delineate drainage areas of major river basins, to assess regional average trends and their statistical significance based on the Mann–Kendall trend test (Mann 1945; Kendall 1975). To characterize the magnitude of changes relative to the range of variability of a historic baseline, we calculated annual z scores of ETo based on a 1980–2000 baseline and calculated the trend in z scores to quantify total change over the study period in units of standard deviations. Regional scale analyses were conducted in R using the *zyp* (Bronaugh and Werner 2019) and *Kendall* (McLeod 2011) packages for slope and trend test calculations, respectively. Finally, we calculated annual values of the four climate variables used to calculate ETo and spatially averaged these within the 18 water resource regions and assessed their trends using the same methods.

c. Sensitivity assessment

We conducted a sensitivity assessment to identify which climate variables contribute the most to ETo trends and how the contributions of individual variables vary regionally and among datasets. Spatially averaged daily data for each water resource region and dataset were used for this analysis. Following methods in McEvoy et al. (2020), we calculated the daily climatologies for each ETo driver as the 1980–2020 average for each day of the year. We then calculated daily ETo four times for each dataset and water resource region, using the actual daily data for one of the four drivers (temperature, wind speed, humidity, incoming solar) while holding the remaining three variables at their respective daily climatologies. We then aggregated daily ETo calculations to annual and seasonal sums and calculated the Theil–Sen slope estimator for each of the iterations. The slope of each ETo calculation iteration provides an indication of the contribution, or sensitivity, of the ETo trend to the variable that was allowed to vary.

3. Results

a. Trend assessment

Most of the CONUS exhibits positive trends in ETo, with the largest and most robust increases occurring in the southwestern United States where ETo increased by a total of 125–250 mm during 1980–2020 (Fig. 1). Much of western CONUS observed at least a 50 mm increase in ETo between 1980 and 2020, while overall change tended to be smaller for

the eastern regions. Only the northernmost parts of the central United States showed relatively consistent negative trends in ETo. Assessment of trends based on z scores conditioned to a 1980–2000 baseline period (Fig. 2) provides additional context for understanding the magnitude of changes, with most of the CONUS exhibiting a two standard deviation increase in ETo. Exceptions to this include the Southwest, where changes were larger and on the order of three standard deviations and in the north-central and central United States where changes were smaller and on the order of ± 1 standard deviation.

Despite most datasets indicating increasing ETo trends across most of the United States, estimates of trends varied considerably among datasets, amounting to large spread in total change over the 41-yr study period. For example, the range of trend magnitudes in regions with the greatest agreement, such as California and the Lower Colorado River, still exceeds 50 mm total change, while the range of trend magnitudes for the region with the widest disagreement among ETo trends calculated from different datasets, the Lower Mississippi, exceeds 185 mm of total change. Overall, there is greater agreement among datasets in the western United States than in the central and eastern United States (as indicated by the standard deviation map in Fig. 1). In some cases, large differences among datasets are driven by regional outliers. For example, NLDAS-2 shows larger increases in ETo relative to other datasets in the easternmost regions (1–9; Fig. 1) and much smaller trends in ETo in the Upper Colorado and Great Basin regions relative to other datasets. In the south-central and southeastern regions, GridMET, ERA5, and NLDAS-2 show relatively large and statistically significant increases in ETo, while MERRA-2 and JRA-55 indicate almost no trend.

The overall changes (Fig. 3) among datasets for the four drivers of ETo provide additional context for observed changes in ETo and variations among datasets. Warming is evident across all regions and datasets (Fig. 3). Overall changes in temperature between 1980 and 2020 are in the range of 1° – 1.5° C (approximately two standard deviations; see supplemental information SI2) for most regions and datasets but are smaller in the Missouri and Souris–Red–Rainy regions and larger in the interior western regions (Lower and Upper Colorado, Rio Grande, Great Basin). In most regions, overall changes in temperature vary by less than 1° C among datasets. Exceptions include the Pacific Northwest, Upper Colorado, and Great Basin, where the NLDAS-2 dataset indicates anomalously small to slightly negative changes in temperature and in the Great Lakes region, where this dataset indicates anomalously large changes in temperature relative to other datasets.

Unlike temperature trends, trends in specific humidity exhibit distinct regional differences. Trends are consistently positive in the eastern United States, while in the six westernmost regions, specific humidity trends are negative for most datasets (Fig. 3). The exception to this is the Pacific Northwest, where most datasets indicate increases in specific humidity. Functionally, the consistency of temperature trends and differences in specific humidity trends between the eastern

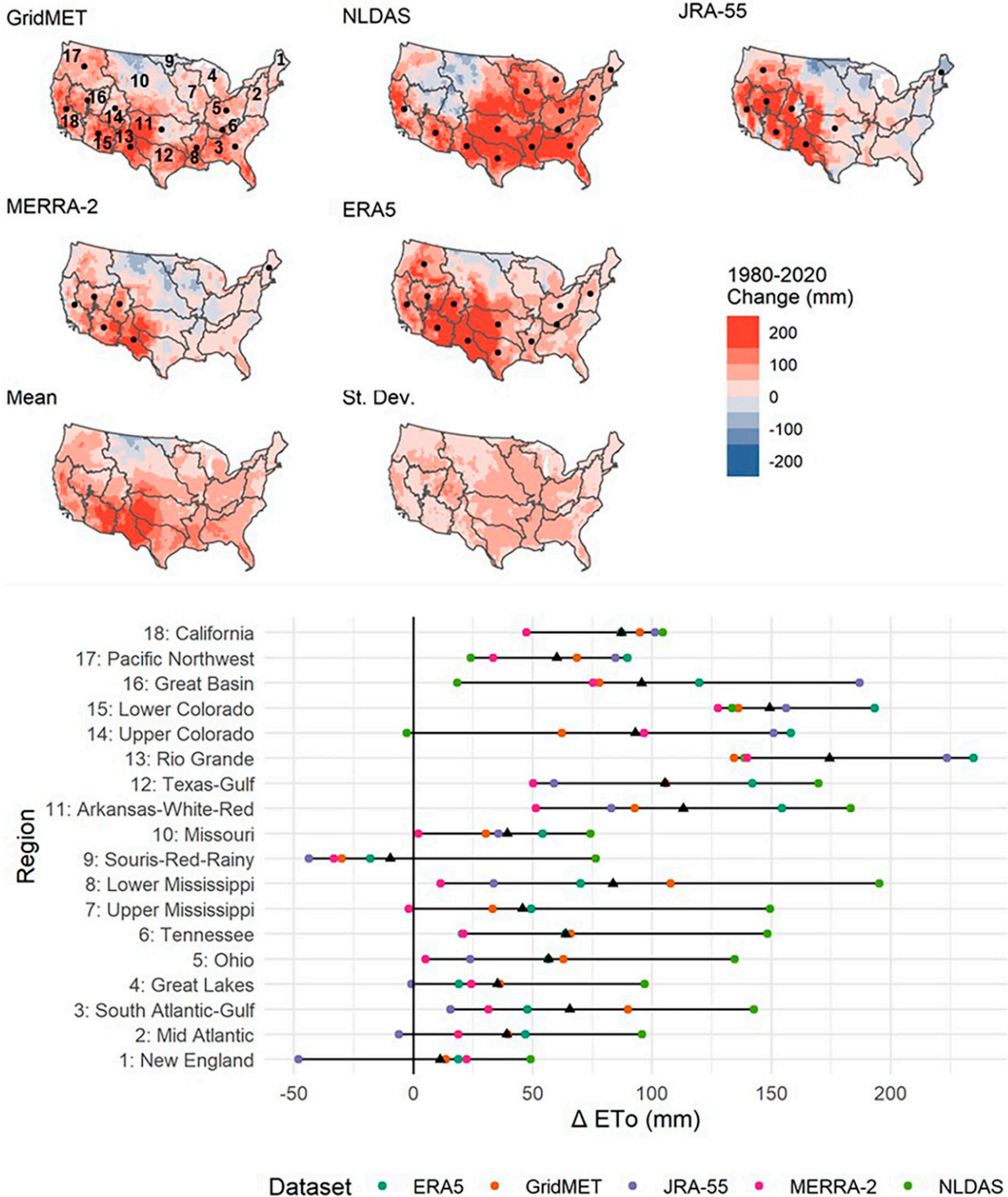


FIG. 1. Total change in reference evapotranspiration (ETo) from 1980 to 2020 (mm) by dataset. Change is calculated as the trend slope based on Sen's slope estimator multiplied by 41 years for each grid cell. Black dots on the map indicate USGS water resource regions, outlined in gray, in which the trend of spatially averaged annual data is statistically significant ($p < 0.05$) based on the Mann-Kendall trend test. Points on the chart indicate the total change as a spatial average for each water resource region for each dataset. Black triangles in the chart indicate the average change among all datasets.

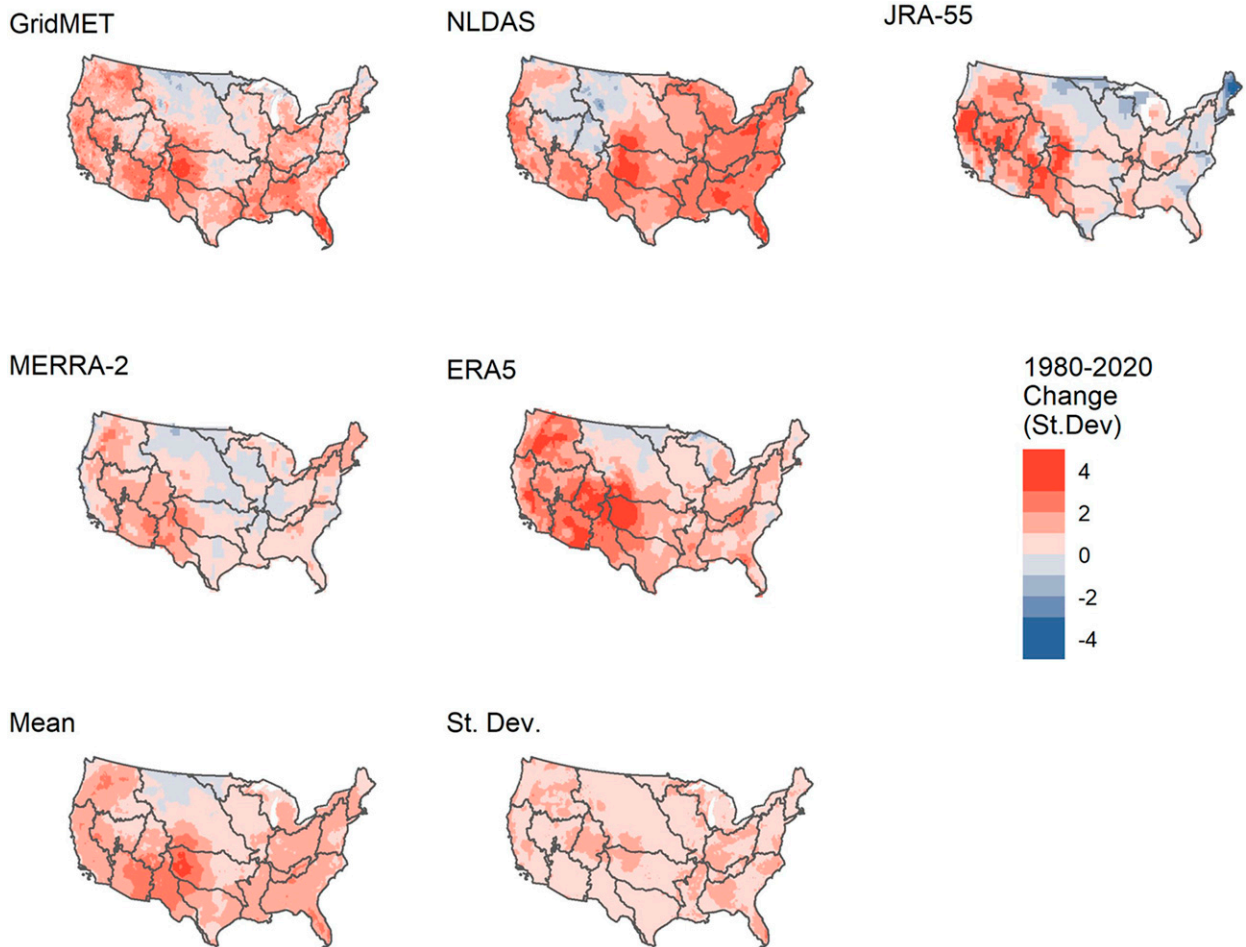


FIG. 2. Total change in reference evapotranspiration (ET₀) from 1980 to 2020 in units of standard deviations, by dataset. The z scores are calculated for each year based on a 1980–2000 baseline mean and standard deviation for each grid cell. The trend slope of the z scores is then calculated based on the Sen's slope estimator for each grid cell and multiplied by the number of years ($n = 41$) to get overall change in units of standard deviations.

and western United States result in differences in trends in vapor pressure deficit. In the case of most western U.S. regions, increases in temperature and decreases in specific humidity both serve to increase vapor pressure deficit, which increases ET₀. In the case of many eastern U.S. regions, increases in both temperature and specific humidity result in much smaller (and in some cases no) increases in vapor pressure deficit (supplemental information SI3), and thus smaller increases in ET₀. Changes in specific humidity among datasets show general agreement (Fig. 3), though MERRA-2 and ERA5 show consistent biases toward more positive and more negative trends, respectively, across most regions.

Regional differences between the western and eastern United States were also observed for wind speed (Fig. 3). Neutral to positive wind speed trends are consistently observed in the same six westernmost regions where specific humidity trends are mostly negative. Changes in wind speed in these regions range between 0 and 0.5 m s^{-1} in total between 1980 and 2020. East of the Rio Grande, trends in wind speed tend to be less

consistent among datasets and are smaller, on average, as JRA-55 indicates more negative wind speed trends for most regions, NLDAS-2 consistently indicates positive wind speed trends, and trends based on MERRA-2 and ERA5 are close to zero.

Incoming surface solar radiation trends exhibit different regional patterns than specific humidity and wind speed, with the greatest and most robust increases in the south central and southwestern regions, on the order of $2.5\text{--}10 \text{ W m}^{-2}$ in total (Fig. 3). Similar to the case of wind speed trends, there is greater agreement among datasets in the western United States than in the eastern United States. Also notable are dataset differences with widespread large increases in incoming solar in eastern CONUS in NLDAS-2 in contrast to decreases in these regions in JRA-55 and MERRA-2.

b. Sensitivity assessment

Increases in temperature contribute substantially toward positive annual ET₀ trends in all regions, accounting for 57% of the increase in ET₀, on average, with humidity, wind speed,

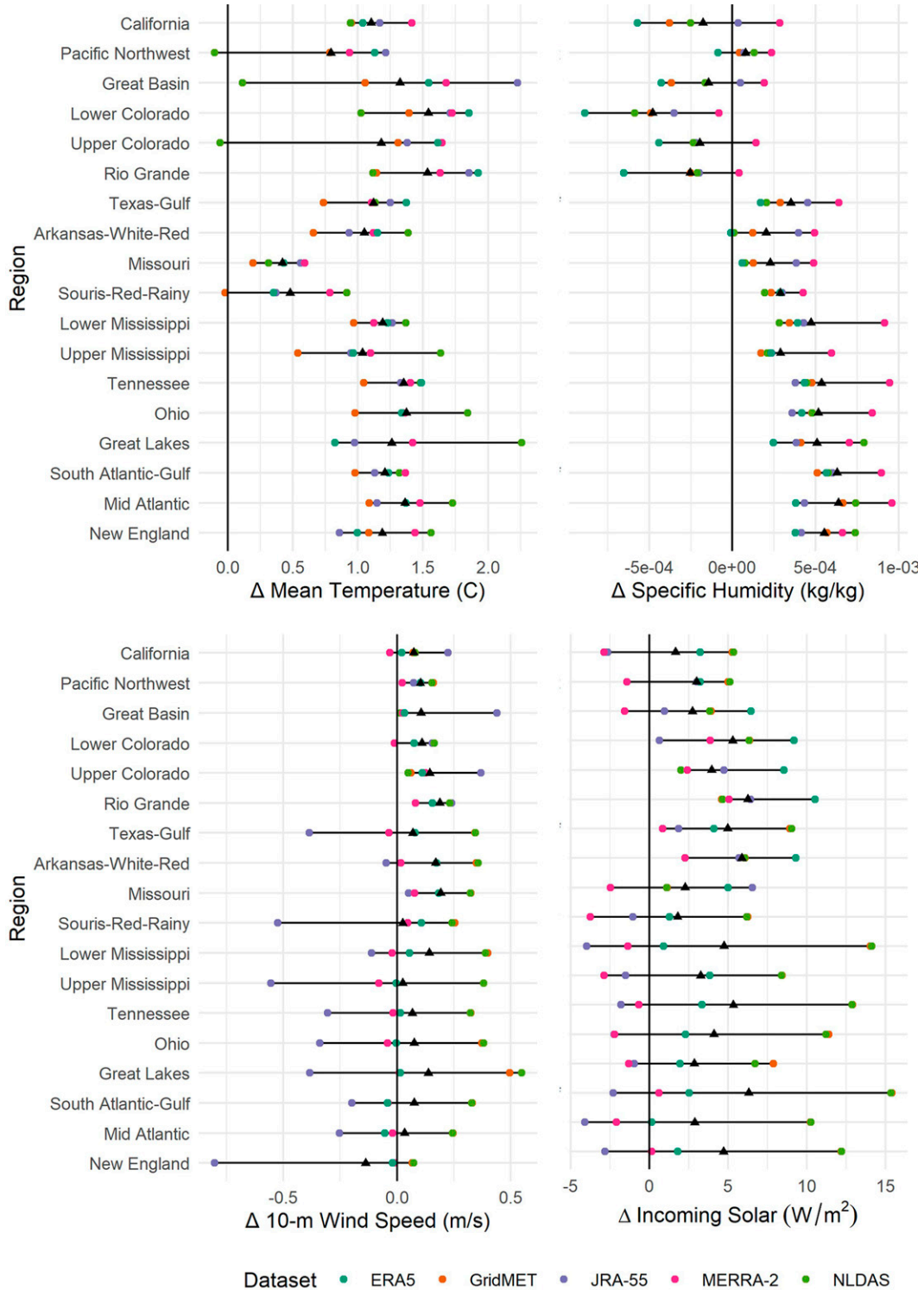


FIG. 3. Total change in annual values of each climate variable by USGS Water Resource Region and dataset. Trends in spatially averaged annual averages of each variable were calculated for each region and multiplied by 41 years. Black triangles indicate the average change among datasets.

and solar radiation accounting for 26%, 10%, and 8% of trends, on average, accordingly. Despite increased temperatures in the eastern United States, concomitant increases in humidity play a strong attenuating role on both vapor pressure deficit and ETo trends, (Fig. 4; supplemental information SI3–5), which is not surprising given that temperature and specific humidity can be strongly correlated in places where water is generally not limiting, such as in much of eastern CONUS (Gaffen and Ross 1999). For example, in the more northern regions of the East, represented by New England and the Great Lakes, increases in humidity counteract the effects of increasing temperature on ETo resulting in little to no trend in ETo. This neutralization effect also occurs in the southeastern United States, as represented by the South Atlantic–Gulf region in Fig. 4, but to a lesser degree. In all three of the eastern U.S. regions the contributions of temperature and humidity to ETo trends are greatest in the case of the NLDAS-2 dataset.

In the western U.S. regions, increases in temperature coupled with decreases in humidity result in increases in vapor pressure deficit, and in turn, ETo everywhere except for the Pacific Northwest, where positive humidity trends slightly attenuate positive trends in ETo. In the Rio Grande region of the Southwest where ETo trends are the largest, all four drivers contribute toward increases in ETo and this pattern is robust across multiple datasets. This is also the case for the Arkansas–White–Red region but to a lesser degree as ETo trends are smaller and there is less agreement on driver contributions among datasets. Also notable in the western United States is the lack of temperature increases in the Upper Colorado in the NLDAS-2 dataset, which contrasts with the large increases observed in other datasets. The lack of increased temperature in the NLDAS-2 dataset is also observed in the Pacific Northwest as well as the Great Basin (supplemental information SI4 and SI5).

Overall, solar radiation trends appear to have limited influence on ETo trends relative to other variables, but play the strongest role in the southern regions, and especially in the Southeast where solar radiation contributes 10%–12% toward overall trends (Fig. 4; supplemental information SI4 and SI5). Trends in wind speed similarly have a more limited influence on ETo trends relative to temperature and humidity but play a stronger role in southern regions than in northern regions and are most influential in the central and interior western U.S. regions where increased wind speed contributes 12%–22% toward overall trends (Fig. 4; supplemental information SI4 and SI5). In the cases where trends in wind and solar radiation are influential, they predominantly contribute toward increases in ETo, with few exceptions (Fig. 4).

Seasonal differences in ETo trends and drivers for each region are shown in Fig. 5. The most striking feature of the map is the strong seasonality of trends in the Rio Grande region, with larger changes in ETo during spring and summer relative to other times of year. Seasonality of trends is also shown in the Pacific Northwest, California, Upper Colorado, and Rio Grande region results, where winter trends in ETo tend to be smaller, possibly due to smaller increases in

temperature during this time of year relative to other seasons and baseline climatologies that are less conducive to changes in ETo. In the Missouri and Souris–Red–Rainy region, trends are negative in winter and spring and positive in summer and fall. This seasonality contrasts with regions like the Arkansas–White–Red, Great Lakes, and other regions in the Northeast where the seasonal contributions to annual ETo trends are relatively constant across all seasons.

4. Discussion

Changes in ETo across much of the United States are on the order of two to three standard deviations from the 1980–2000 baseline, indicating they are emerging outside the range of variability of that era. The largest and most robust increases in ETo occurred in the southwestern United States, roughly centered on the Rio Grande and the Lower Colorado, with increases in ETo of 135–235 mm. Although these southwestern regions exhibit slightly larger temperature changes relative to elsewhere in the CONUS, complementary changes in other variables—increased wind speed, increased incoming solar radiation, and decreased specific humidity—exacerbated ETo increases in these regions, and are responsible for about 10%–40% of the observed change, depending on the dataset analyzed (supplemental information SI4).

Crop water requirements are most commonly estimated using ETo (Allen et al. 1998). To put the changes in the Rio Grande in perspective from the standpoint of crop water requirements, a 135–235 mm ETo change represents an 8%–15% increase from 1980 meaning that 8%–15% more water is needed to maintain a well-watered crop on the same amount of land area in 2020 relative to 1980, assuming no other changes in management. These increases in crop water requirements are coincident with declining runoff ratios on the Rio Grande due to warming temperatures and increased evaporative losses (Lehner et al. 2017), representing a compounding stress on water supplies. This result agrees with previous studies that have shown aridification of the southwestern region (Milly and Dunne 2020; McCabe et al. 2017; Udall and Overpeck 2017; Dettinger et al. 2015). We additionally show here that recent annual ETo lies outside the range experienced in the late twentieth century, that this result is robust across multiple climate datasets, and that this is driven by multiple trends in climatic variables that are likely resulting from both natural variability and temperature-driven shifts in the climate system. The degree to which these changes are attributable to anthropogenic climate forcing and natural variability are beyond the scope of this analysis, although previous studies have shown that anthropogenic forcing has played a dominant role (Williams et al. 2020).

Despite relatively consistent changes in temperature of 1°–1.5°C in most regions, we found considerable differences between the eastern and western United States. ETo trends due to large increases in specific humidity in the eastern United States served to dampen, but not completely eliminate, increases in vapor pressure deficit and ETo. Regional disparities in ETo trends are further driven by declines in specific humidity in many western regions, consistent with

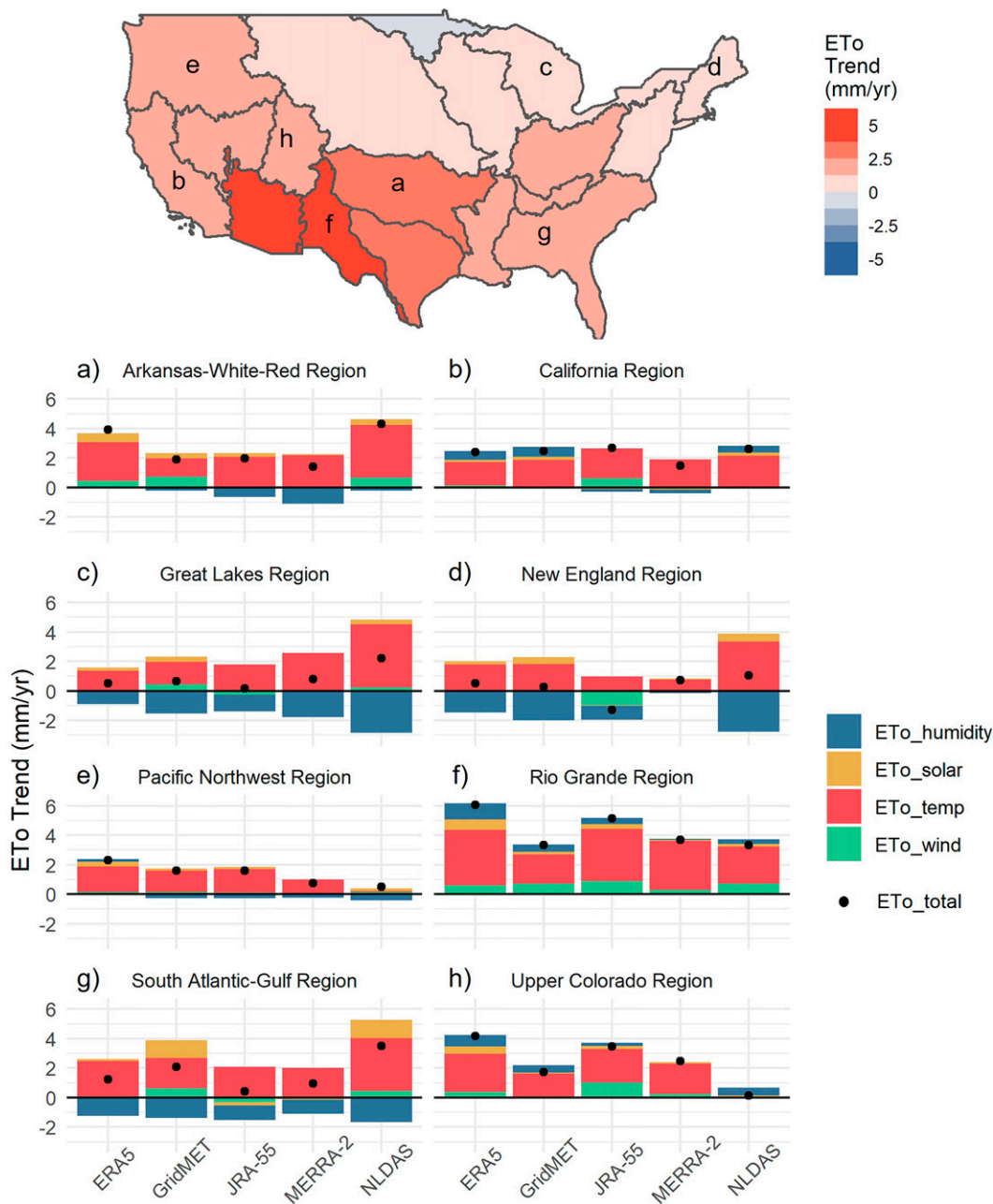


FIG. 4. (top) Average trend slope (change per year) of reference evapotranspiration (ETo) across all datasets and by water resource region; (a)–(h) the contribution of individual drivers to observed ETo trends by dataset, as determined through sensitivity analysis, for select regions. The black dots indicate the spatially averaged ETo trend for each region and dataset as a point of reference. Bar plots for the 10 other regions not shown here can be found in supplemental information SI5.

McKinnon et al. (2021), leading to greater increases in vapor pressure deficit and ETo. The degree to which recent increases in humidity in the East and decreases in humidity in the West are driven by large-scale climate patterns versus localized land–atmosphere feedbacks is unclear and notoriously difficult to tease apart (Vicente-Serrano et al. 2018; Bishop et al. 2021) but both factors are likely at play. For

example, the observed increases in the eastern United States are consistent with land–atmosphere feedbacks and the complementary relationship of evaporation (Bouchet 1963; Brutsaert 1982), whereby under non-water-limited conditions, ETo and actual evapotranspiration (ETa) are expected to converge as atmospheric demand for water is met by additional water provided by increased ETa, thereby lowering

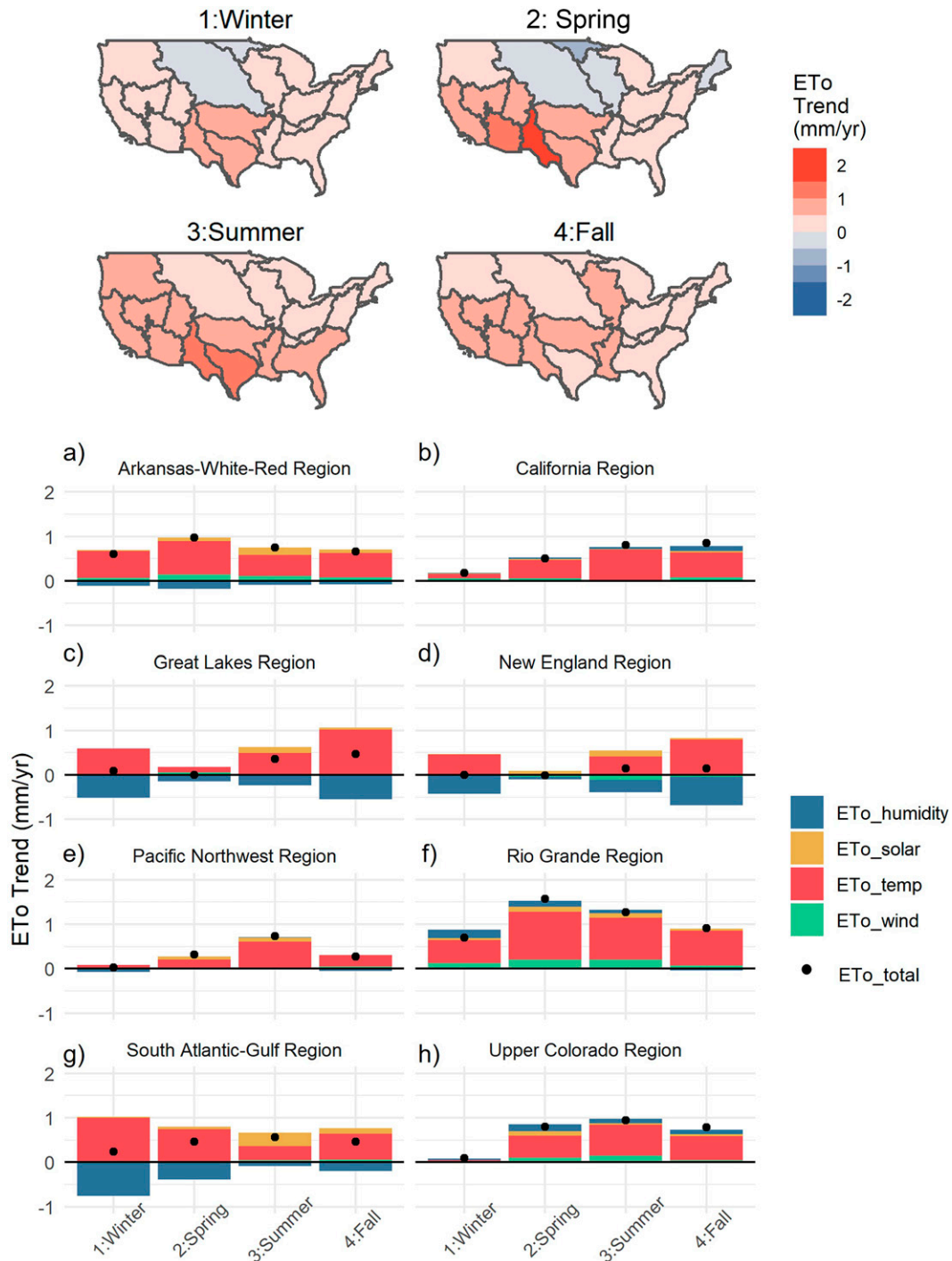


FIG. 5. (top) Average trend slope (change per year) of reference evapotranspiration (ETo) across all datasets by season and water resource region; (a)–(h) the average contribution of individual drivers to observed ETo trends by season, as determined through sensitivity analysis, for select regions (see Fig. 4 for map locations). The black dots indicate the spatially averaged ETo trend for each quarter and region. Bar plots for the 10 other regions not shown here can be found in supplemental information S16.

ETo. Observed increases in ETa in this region (Jasinski et al. 2019) may be further enhanced by agricultural intensification in places like the central United States (Brown and

Degaetano 2013). At the same time, the recent dominance and amplification of the North American winter dipole (Singh et al. 2016), which has been connected to warmer and drier

winters in the western United States and cooler and wetter patterns in the East, may explain the east–west divergence of trends in humidity, in part.

In water-limited regions, complementary theory predicts a positive feedback, as increases in ETo are met with decreases in ETa due to lack of surface and soil water availability, which results in increases in sensible heat flux that further increase temperature and vapor pressure deficits, and in turn ETo. While decreases in specific humidity are observed throughout the water-limited West, these changes are relatively small and may be tied to shifts in precipitation patterns and atmospheric circulation as there has been a weak negative trend in precipitation in the West (Singh et al. 2016). Decreases in humidity in the arid Southwest have also been observed in association with decreases in ETa, possibly due to the negative trend in precipitation and more rapid depletion of soil moisture earlier in the season caused by warming temperatures (McKinnon et al. 2021), suggesting a detectable role of land–atmosphere feedbacks and the complementary relationship of evaporation. The relative roles and seasonal timing of these processes—and how well they are represented in climate model projections—is an important question looking forward. McEvoy et al. (2020) conducted a similar study of ETo trends in California and Nevada based on future climate projections. That study showed increases in specific humidity, which helped to dampen temperature-driven increases in ETo, contrary to the recent historical trends reported here for most datasets. The reason for this difference is unclear, but merits further investigation.

The sensitivity assessment conducted in this study highlights regional differences in drivers of ETo trends with temperature and humidity playing dominant roles. While there is great potential for ETo to exhibit sensitivities to wind and solar radiation (Hobbins 2016; Nouri et al. 2017; McVicar et al. 2012) these variables were less influential on trends over the time period analyzed in this study. This may be due to the more cyclical nature of these variables during the time period analyzed. For example, solar radiation across the CONUS exhibited a brightening trend from the early 1980s to 2012 and has since been on a dimming trajectory associated with recent increases in cloud cover (Augustine et al. 2019). Winds in North America have also exhibited a cyclical pattern with increases in wind speeds occurring between 1980 and 1990, decreases during 1990–2010, and a rapid increase beginning around 2011 (Zeng et al. 2019). Fan et al. (2021) found that, as compared to ground observations, all reanalysis datasets underestimated trends in wind speeds in North America during the 1990–2018 time period, indicating that the lack of strong sensitivity of ETo trends to wind (and possibly also solar radiation) observed in this study could also be due to the inability of these datasets to accurately represent trends in these variables.

Examining sensitivity of ETo trends to its drivers from a seasonal perspective, it is clear that most western United States regions and some southern regions exhibit seasonality in ETo trends, with larger changes occurring during spring, summer, and fall, and smaller changes during winter, consistent with VPD changes observed in Ficklin and Novick

(2017). The robust degree of change in ETo observed across the West—on the order of two to three standard deviations from the 1980–2000 baseline—during the already most water-limited seasons is consistent with ecological changes that are now being observed, including widespread tree mortality (Williams et al. 2013; Breshears et al. 2013), enhanced forest fire activity (Williams et al. 2014, 2015; Abatzoglou and Williams 2016; Abatzoglou et al. 2021), and reduced streamflows (Das et al. 2011; McCabe et al. 2017) that are associated with warm season changes in atmospheric water demand.

Although most CONUS regions exhibited increases in ETo, on average, we found substantial differences in both the direction and magnitude of ETo trends across large portions of the central and eastern United States especially, underscoring the utility and importance of conducting such assessments using an ensemble of datasets. Disagreement among datasets on the direction and magnitude of ETo trends are most strongly driven by NLDAS-2 and JRA-55. In contrast to all other datasets assessed in this study as well as a wealth of studies in the Upper Colorado River basin (Udall and Overpeck 2017; McCabe et al. 2017) and other parts of the West (Vose et al. 2012), NLDAS-2 exhibits no trend in mean annual temperature in the Pacific Northwest, Great Basin, and Upper Colorado. This dataset also shows anomalous temperature and solar radiation increases relative to other datasets in the central and eastern United States. A possible reason for the temperature differences is that, unlike other reanalysis products, the forcing data for NLDAS-2 and NARR, do not assimilate near-surface observations of temperature (Mesinger et al. 2006). In the eastern United States, our result is consistent with Grotjahn and Huynh (2018), which showed that NARR-based maximum temperature trends tended to be larger relative to other reanalysis datasets. In the case of JRA-55, anomalously large declines in wind speeds in the central and eastern United States appear to explain differences between this dataset and others in terms of resultant ETo trends. The findings in this paper have important implications for operational satellite remote sensing and long-term trend assessments of ETa model ensembles (e.g., Melton et al. 2022), given the strong reliance of ETa models on gridded climate products and ETo.

The datasets analyzed in this study provide valuable, albeit imperfect, representations of variations in the land surface water and energy balance over extended periods of time in places where long-term in situ observations are lacking. And although inconsistencies in trends are observed, the five datasets analyzed were consistent in capturing interannual variability in temperature and humidity, as indicated by high average correlations among datasets, which translates to high correlations in ETo among datasets (supplemental information SI7 and SI8). There is less agreement in trends of solar radiation and winds, especially in the central and eastern United States, and correlations among datasets are considerably lower for these variables (supplemental information SI7). Observations of wind and solar radiation are more limited relative to temperature and humidity and notably do not tend to be derived from observations at the land surface. For example, wind speeds are most commonly derived from

upper-air measurements and satellite observations (Fan et al. 2021), while solar radiation is estimated based on a radiative transfer model rather than on assimilation of direct measurements (Boilley and Wald 2015). In the case of wind speed, reanalysis products commonly show large biases, especially in the eastern United States (Carvalho 2019), and trends do not match those seen in ground observations (Fan et al. 2021). Biases and errors in solar radiation variables in reanalysis and derivative products such as NLDAS-2 are also well acknowledged (Slater 2016; Urraca et al. 2018; Boilley and Wald 2015), suggesting a need for improvement of observation networks as well as approaches to data assimilation and bias correction (Slater 2016).

5. Conclusions

In this study, we conducted a systematic CONUS-wide assessment of recent (1980–2020) trends in annual ETo and its drivers with five gridded datasets that are commonly used for climatological studies. In doing so, we illustrate large and robust changes in ETo on the order of two to three standard deviations from the 1980–2000 baseline across much of the western United States, and centered on the southwestern United States, indicating that current conditions are emerging outside the range of variability experienced 20–40 years ago. We further identify regional and seasonal differences in the climatic drivers of these trends, highlighting the strong influence of temperature in all regions, the mitigating role of specific humidity on ETo increases in non-water-limited regions, and the smaller but still substantial impacts of decreased specific humidity, increased wind speed, and increased incoming solar radiation on ETo increases across various areas of the CONUS. Finally, we characterize the structural uncertainties in trends of ETo finding greater disagreement among datasets in the central and eastern United States as well as the Upper Colorado River basin and surrounding areas. In the latter region, a large disparity between temperature trends in NLDAS-2 and other datasets are driving ETo differences, while large solar radiation, wind, and, to a lesser degree, temperature trend differences among datasets are contributing to greater uncertainties in ETo trends farther to the east. Results from this analysis provide new insights into patterns of ETo trends across CONUS, and the potential implications of researchers' choice of climate datasets for retrospective climate impact analyses.

Perhaps more importantly, this analysis and intercomparison indicates atmospheric demands far exceed what was observed in the 1980s across most of the western United States. This means that crops require more water now than in the past, year in and year out, and can reliably be expected to require more water now and, presumably, the future. These higher evaporative demands mean that, for every drop of precipitation that falls, less water is likely to drain into streams, wetlands, and aquifers across the region. Soils and vegetation spend more time in drier conditions, increasing potential for forest fire, tree mortality, and tree regeneration failure. Essentially, these changes have long been expected as a consequence of recent regional warming trends and ultimately

global warming; this study finds that such changes already have been large and that, although projections of these trends have mostly been based on temperature considerations, the changes to date are 1) reflections of trends in a whole range of interconnected climate variables—albeit most prominently, temperature, and 2) are robust across a number of modern data sources. These amplified evaporative demands constitute a new and apparently persistent forcing of western landscapes and water supplies toward drought. Land and water managers, policy makers and public alike, need to recognize that this enhanced demand-side aspect of drought (and “flash drought”) is a historically large contributor to twenty-first-century western droughts, and if the trends continue will too soon become the new face of many future droughts.

Acknowledgments. This research was funded by the Sulo and Aileen Maki Endowment Fund to the Desert Research Institute's Division of Hydrologic Sciences, the National Oceanic and Atmospheric Administration (NOAA) California–Nevada Climate Applications Program (NA17OAR4310284), NOAA National Integrated Drought Information System California–Nevada Drought Early Warning System (NA20OAR4310253C), the NASA Applied Sciences, Water Resources Program (NNX17AF53G), the U.S. Geological Survey Landsat Science Team (140G0118C0007), and USDA-NIFA project (2021-69012-35916).

Data availability statement. Data analyzed in this study are openly available at locations cited in the reference section.

REFERENCES

- Abatzoglou, J. T., 2013: Development of gridded surface meteorological data for ecological applications and modelling. *Int. J. Climatol.*, **33**, 121–131, <https://doi.org/10.1002/joc.3413>.
- , and C. A. Kolden, 2013: Relationships between climate and macroscale area burned in the western United States. *Int. J. Wildland Fire*, **22**, 1003–1020, <https://doi.org/10.1071/WF13019>.
- , and A. P. Williams, 2016: Impact of anthropogenic climate change on wildfire across western US forests. *Proc. Natl. Acad. Sci. USA*, **113**, 11 770–11 775, <https://doi.org/10.1073/pnas.1607171113>.
- , C. S. Juang, A. P. Williams, C. A. Kolden, and A. L. R. Westerling, 2021: Increasing synchronous fire danger in forests of the western United States. *Geophys. Res. Lett.*, **48**, e2020GL091377, <https://doi.org/10.1029/2020GL091377>.
- Allen, R. G., L. S. Pereira, D. Raes, and M. Smith, 1998: Crop evapotranspiration: Guidelines for computing crop water requirements. FAO Irrigation and Drainage Paper 56, 300 pp., <http://www.fao.org/3/X0490E/X0490E00.htm>.
- , I. Walter, R. Elliott, T. Howell, D. Itenfisu, M. Jensen, and R. Snyder, 2005: *The ASCE Standardized Reference Evapotranspiration Equation*. American Society of Civil Engineers, 59 pp.
- Alter, R. E., H. C. Douglas, J. M. Winter, and E. A. B. Eltahir, 2018: Twentieth century regional climate change during the summer in the Central United States attributed to

- agricultural intensification. *Geophys. Res. Lett.*, **45**, 1586–1594, <https://doi.org/10.1002/2017GL075604>.
- Andreadis, K. M., and D. P. Lettenmaier, 2006: Trends in 20th century drought over the continental United States. *Geophys. Res. Lett.*, **33**, L10403, <https://doi.org/10.1029/2006GL025711>.
- Augustine, J. A., G. B. Hodges, N. Global, and E. Sciences, 2019: Variability of surface radiation budget components over the U.S. from 1996 to 2019—Has brightening ceased? *J. Geophys. Res. Atmos.*, **126**, e2020JD033590, <https://doi.org/10.1029/2020JD033590>.
- Bishop, D. A., A. P. Williams, R. Seager, E. R. Cook, D. M. Peteet, B. I. Cook, M. P. Rao, and D. W. Stahle, 2021: Placing the east-west North American aridity gradient in a multi-century context. *Environ. Res. Lett.*, **16**, 114043, <https://doi.org/10.1088/1748-9326/ac2f63>.
- Boilley, A., and L. Wald, 2015: Comparison between meteorological re-analyses from ERA-Interim and MERRA and measurements of daily solar irradiation at surface. *Renewable Energy*, **75**, 135–143, <https://doi.org/10.1016/j.renene.2014.09.042>.
- Bouchet, R., 1963: Évapotranspiration réelle et potentielle, signification climatique. *IAHS Publ.*, **62**, 134–142.
- Breshears, D. D., H. D. Adams, D. Eamus, N. G. McDowell, D. J. Law, R. E. Will, A. P. Williams, and C. B. Zou, 2013: The critical amplifying role of increasing atmospheric moisture demand on tree mortality and associated regional die-off. *Front. Plant Sci.*, **4**, 2–5, <https://doi.org/10.3389/fpls.2013.00266>.
- Bronaugh, D., and A. T. Werner, 2019: zyp: Zhang + Yue-Pilon Trends Package, version 0.10-1.1. R package, <https://rdr.io/cran/zyp/>.
- Brown, P. J., and A. T. Degaetano, 2013: Trends in U.S. surface humidity, 1930–2010. *J. Appl. Meteor. Climatol.*, **52**, 147–163, <https://doi.org/10.1175/JAMC-D-12-035.1>.
- Brutsaert, W., 1982: *Evaporation into the Atmosphere Theory, History, and Applications*. 1st ed. Springer, 299 pp.
- Carvalho, D., 2019: An assessment of NASA's GMAO MERRA-2 reanalysis surface winds. *J. Climate*, **32**, 8261–8281, <https://doi.org/10.1175/JCLI-D-19-0199.1>.
- Condon, L. E., A. L. Atchley, and R. M. Maxwell, 2020: Evapotranspiration depletes groundwater under warming over the contiguous United States. *Nat. Commun.*, **11**, 873, <https://doi.org/10.1038/s41467-020-14688-0>.
- Cosgrove, B. A., and Coauthors, 2003: Real-time and retrospective forcing in the North American Land Data Assimilation System (NLDAS) project. *J. Geophys. Res.*, **108**, 8842, <https://doi.org/10.1029/2002JD003118>.
- Daly, C., and Coauthors, 2008: Physiographically sensitive mapping of climatological temperature and precipitation across the conterminous United States. *Int. J. Climatol.*, **28**, 2031–2064, doi:10.1002/joc.1688.
- Das, T., D. W. Pierce, D. R. Cayan, J. A. Vano, and D. P. Lettenmaier, 2011: The importance of warm season warming to western U.S. streamflow changes. *Geophys. Res. Lett.*, **38**, L23403, <https://doi.org/10.1029/2011GL049660>.
- Dennison, P., S. C. Brewer, J. D. Arnold, and M. A. Moritz, 2014: Large wildfire trends in the western United States, 1984–2011. *Geophys. Res. Lett.*, **41**, 2928–2933, <https://doi.org/10.1002/2014GL059576>.
- Dettinger, M., B. Udall, and A. Georgakakos, 2015: Western water and climate change. *Ecol. Appl.*, **25**, 2069–2093, <https://doi.org/10.1890/15-0938.1>.
- Diffenbaugh, N. S., D. L. Swain, D. Touma, and J. Lubchenco, 2015: Anthropogenic warming has increased drought risk in California. *Proc. Natl. Acad. Sci. USA*, **112**, 3931–3936, <https://doi.org/10.1073/pnas.1422385112>.
- Fan, W., Y. Liu, A. Chappell, L. Dong, R. Xu, M. Ekström, T.-M. Fu, and Z. Zeng, 2021: Evaluation of global reanalysis land surface wind speed trends to support wind energy development using in situ observations. *J. Appl. Meteor. Climatol.*, **60**, 33–50, <https://doi.org/10.1175/JAMC-D-20-0037.1>.
- Feng, S., and Q. Fu, 2013: Expansion of global drylands under a warming climate. *Atmos. Chem. Phys.*, **13**, 10081–10094, <https://doi.org/10.5194/acp-13-10081-2013>.
- Fettig, C. J., L. A. Mortenson, B. M. Bulaon, and P. B. Foulk, 2019: Tree mortality following drought in the central and southern Sierra Nevada, California, U.S. *For. Ecol. Manage.*, **432**, 164–178, <https://doi.org/10.1016/j.foreco.2018.09.006>.
- Ficklin, D. L., and K. A. Novick, 2017: Historic and projected changes in vapor pressure deficit suggest a continental-scale drying of the United States atmosphere. *J. Geophys. Res.*, **122**, 2061–2079, <https://doi.org/10.1002/2016JD025855>.
- , J. T. Maxwell, S. L. Letsinger, and H. Gholizadeh, 2015: A climatic deconstruction of recent drought trends in the United States. *Environ. Res. Lett.*, **10**, 044009, <https://doi.org/10.1088/1748-9326/10/4/044009>.
- , S. M. Robeson, and J. H. Knouft, 2016: Impacts of recent climate change on trends in baseflow and stormflow in United States watersheds. *Geophys. Res. Lett.*, **43**, 5079–5088, <https://doi.org/10.1002/2016GL069121>.
- Fisher, J. B., R. J. Whittaker, and Y. Malhi, 2011: ET come home: Potential evapotranspiration in geographical ecology. *Global Ecol. Biogeogr.*, **20**, 1–18, <https://doi.org/10.1111/j.1466-8238.2010.00578.x>.
- Gaffen, D. J., and R. J. Ross, 1999: Climatology and trends of U.S. surface humidity and temperature. *J. Climate*, **12**, 811–828, [https://doi.org/10.1175/1520-0442\(1999\)012<0811:CATOUS>2.0.CO;2](https://doi.org/10.1175/1520-0442(1999)012<0811:CATOUS>2.0.CO;2).
- Gelaro, R., and Coauthors, 2017: The Modern-Era Retrospective Analysis for Research and Applications, version 2 (MERRA-2). *J. Climate*, **30**, 5419–5454, <https://doi.org/10.1175/JCLI-D-16-0758.1>.
- Global Modeling and Assimilation Office, 2015: MERRA-2 tavg1_2d_flux_Nx: 2d,1-Hourly, Time-Averaged, Single-Level, Assimilation, Surface Flux Diagnostics V5.12.4. GES DISC, accessed 15 January 2021, https://disc.gsfc.nasa.gov/datasets/M2T1NXFLX_5.12.4/summary.
- Gorelick, N., M. Hancher, M. Dixon, S. Ilyushchenko, D. Thau, and R. Moore, 2017: Google Earth Engine: Planetary-scale geospatial analysis for everyone. *Remote Sensing Environ.*, **202**, 18–27, <https://doi.org/10.1016/j.rse.2017.06.031>.
- Groisman, P. Ya., R. W. Knight, T. R. Karl, D. R. Easterling, B. Sun, and J. H. Lawrimore, 2004: Contemporary changes of the hydrological cycle over the contiguous United States: Trends derived from in situ observations. *J. Hydrometeorol.*, **5**, 64–85, [https://doi.org/10.1175/1525-7541\(2004\)005<0064:CCOTHC>2.0.CO;2](https://doi.org/10.1175/1525-7541(2004)005<0064:CCOTHC>2.0.CO;2).
- Grossiord, C., T. N. Buckley, L. A. Cernusak, K. A. Novick, B. Poulter, R. T. W. Siegwolf, J. S. Sperry, and N. G. McDowell, 2020: Plant responses to rising vapor pressure deficit. *New Phytol.*, **226**, 1550–1566, <https://doi.org/10.1111/nph.16485>.
- Grotjahn, R., and J. Huynh, 2018: Contiguous US summer maximum temperature and heat stress trends in CRU and NOAA Climate Division data plus comparisons to

- reanalyses. *Sci. Rep.*, **8**, 11146, <https://doi.org/10.1038/s41598-018-29286-w>.
- Hersbach, H., and Coauthors, 2018: ERA5 hourly data on single levels from 1979 to present. Copernicus Climate Data Store, accessed 4 June 2021, <https://cds.climate.copernicus.eu/cdsapp#!/dataset/reanalysis-era5-single-levels?tab=overview>.
- , and Coauthors, 2020: The ERA5 global reanalysis. *Quart. J. Roy. Meteor. Soc.*, **146**, 1999–2049, <https://doi.org/10.1002/qj.3803>.
- Hobbins, M., and J. L. Huntington, 2016: Evapotranspiration and evaporative demand. *Handbook of Applied Hydrology*, V. Singh, Ed., McGraw-Hill Publishing, 42.1–42.18.
- Hobbins, M. T., 2016: The variability of ASCE Standardized reference evapotranspiration: A rigorous, CONUS-wide decomposition and attribution. *Trans. ASABE*, **59**, 561–576, <https://doi.org/10.13031/trans.59.10975>.
- , J. A. Ramírez, and T. C. Brown, 2004: Trends in pan evaporation and actual evapotranspiration across the conterminous U.S.: Paradoxical or complementary? *Geophys. Res. Lett.*, **31**, L13503, <https://doi.org/10.1029/2004GL019846>.
- , A. Wood, D. J. McEvoy, J. L. Huntington, C. Morton, M. Anderson, and C. Hain, 2016: The evaporative demand drought index. Part I: Linking drought evolution to variations in evaporative demand. *J. Hydrometeorol.*, **17**, 1745–1761, <https://doi.org/10.1175/JHM-D-15-0121.1>.
- Hobbins, M., D. McEvoy, and C. Hain, 2017: Evapotranspiration, evaporative demand, and drought. *Drought and Water Crises*, D. Wilhite and R. S. Pulwarty, Eds., CRC Press, 259–288.
- Huntington, T. G., 2006: Evidence for intensification of the global water cycle: Review and synthesis. *J. Hydrol.*, **319**, 83–95, <https://doi.org/10.1016/j.jhydrol.2005.07.003>.
- Japan Meteorological Agency, 2013: JRA-55: Japanese 55-year reanalysis, daily 3-hourly and 6-hourly data. Research Data Archive at the National Center for Atmospheric Research, accessed 12 February 2021, <https://doi.org/10.5065/D6HH6H41>.
- Jasinski, M. F., and Coauthors, 2019: NCA-LDAS: Overview and analysis of hydrologic trends for the national climate assessment. *J. Hydrometeorol.*, **20**, 1595–1617, <https://doi.org/10.1175/JHM-D-17-0234.1>.
- Kendall, M. G., 1975: *Rank Correlation Methods*. 4th ed. Charles Griffin, 272 pp.
- Kobayashi, S., and Coauthors, 2015: The JRA-55 reanalysis: General specifications and basic characteristics. *J. Meteor. Soc. Japan*, **93**, 5–48, <https://doi.org/10.2151/jmsj.2015-001>.
- Kramer, R. J., L. Bounoua, P. Zhang, R. E. Wolfe, T. G. Huntington, M. L. Imhoff, K. Thome, and G. L. Noyce, 2015: Evapotranspiration trends over the Eastern United States during the 20th century. *Hydrology*, **2**, 93–111, <https://doi.org/10.3390/hydrology2020093>.
- Lawrimore, J. H., and T. C. Peterson, 2000: Pan evaporation trends in dry and humid regions of the United States. *J. Hydrometeorol.*, **1**, 543–546, [https://doi.org/10.1175/1525-7541\(2000\)001<0543:PETIDA>2.0.CO;2](https://doi.org/10.1175/1525-7541(2000)001<0543:PETIDA>2.0.CO;2).
- Lehner, F., E. R. Wahl, A. W. Wood, D. B. Blatchford, and D. Llewellyn, 2017: Assessing recent declines in Upper Rio Grande runoff efficiency from a paleoclimate perspective. *Geophys. Res. Lett.*, **44**, 4124–4133, <https://doi.org/10.1002/2017GL073253>.
- Mann, H. B., 1945: Nonparametric tests against trend. *Econometrica*, **13**, 245–259, <https://doi.org/10.2307/1907187>.
- McAfee, S. A., 2013: Methodological differences in projected potential evapotranspiration. *Climatic Change*, **120**, 915–930, <https://doi.org/10.1007/s10584-013-0864-7>.
- McCabe, G. J., and D. M. Wolock, 2015: Increasing Northern Hemisphere water deficit. *Climate Change*, **132**, 237–249, <https://doi.org/10.1007/s10584-015-1419-x>.
- , —, G. T. Pederson, C. A. Woodhouse, and S. McAfee, 2017: Evidence that recent warming is reducing Upper Colorado River flows. *Earth Interact.*, **21**, <https://doi.org/10.1175/EI-D-17-0007.1>.
- McCarty, W., L. Coy, R. Gelaro, A. Huang, D. Merkova, E. B. Smith, M. Sienkiewicz, and K. Wargan, 2016: MERRA-2 input observations: Summary and assessment. NASA Rep. NASA/TM–2016-104606/Vol. 46, 51 pp., <https://gmao.gsfc.nasa.gov/pubs/docs/McCarty885.pdf>.
- McEvoy, D. J., J. L. Huntington, M. T. Hobbins, A. Wood, C. Morton, M. Anderson, and C. Hain, 2016: The evaporative demand drought index. Part II: CONUS-wide assessment against common drought indicators. *J. Hydrometeorol.*, **17**, 1763–1779, <https://doi.org/10.1175/JHM-D-15-0122.1>.
- , D. W. Pierce, J. F. Kalansky, D. R. Cayan, and J. T. Abatzoglou, 2020: Projected changes in reference evapotranspiration in California and Nevada: Implications for drought and wildland fire danger. *Earth's Future*, **8**, e2020EF001736, <https://doi.org/10.1029/2020EF001736>.
- McKinnon, K. A., A. Poppick, and I. R. Simpson, 2021: Hot extremes have become drier in the United States Southwest. *Nat. Climate Change*, **11**, 598–604, <https://doi.org/10.1038/s41558-021-01076-9>.
- McLeod, A., 2011: Kendall: Kendall rank correlation and Mann-Kendall trend test, version 2.2. R package, <https://rdrr.io/cran/Kendall/>.
- McVicar, T. R., and Coauthors, 2012: Global review and synthesis of trends in observed terrestrial near-surface wind speeds: Implications for evaporation. *J. Hydrol.*, **416–417**, 182–205, <https://doi.org/10.1016/j.jhydrol.2011.10.024>.
- Melton, F. S., and Coauthors, 2022: OpenET: Filling a critical data gap in water management for the western United States. *J. Amer. Water Resour. Assoc.*, <https://doi.org/10.1111/1752-1688.12956>, in press.
- Mesinger, F., and Coauthors, 2006: North American Regional Reanalysis. *Bull. Amer. Meteor. Soc.*, **87**, 343–360, <https://doi.org/10.1175/BAMS-87-3-343>.
- Milly, P. C. D., and K. A. Dunne, 2016: Potential evapotranspiration and continental drying. *Nat. Climate Change*, **6**, 946–949, <https://doi.org/10.1038/nclimate3046>.
- , and —, 2017: A hydrologic drying bias in water-resource impact analyses of anthropogenic climate change. *J. Amer. Water Resour. Assoc.*, **53**, 822–838, <https://doi.org/10.1111/1752-1688.12538>.
- , and —, 2020: Colorado River flow dwindles as warming-driven loss of reflective snow energizes evaporation. *Science*, **367**, 1252–1255, <https://doi.org/10.1126/science.aax0194>.
- Monteith, J. L., 1965: Evaporation and environment. *Symp. Soc. Exp. Biol.*, **19**, 205–234.
- Mote, P. W., and Coauthors, 2016: Perspectives on the causes of exceptionally low 2015 snowpack in the western United States. *Geophys. Res. Lett.*, **43**, 10980–10988, <https://doi.org/10.1002/2016GL069965>.
- Nouri, M., M. Homaei, and M. Bannayan, 2017: Quantitative trend, sensitivity and contribution analyses of reference evapotranspiration in some arid environments under climate

- change. *Water Resour. Manage.*, **31**, 2207–2224, <https://doi.org/10.1007/s11269-017-1638-1>.
- Pryor, S. C., and Coauthors, 2009: Wind speed trends over the contiguous United States. *J. Geophys. Res.*, **114**, D14105, <https://doi.org/10.1029/2008JD011416>.
- Seager, R., A. Hooks, A. P. Williams, B. Cook, J. Nakamura, and N. Henderson, 2015: Climatology, variability, and trends in the U.S. vapor pressure deficit, an important fire-related meteorological quantity. *J. Appl. Meteor. Climatol.*, **54**, 1121–1141, <https://doi.org/10.1175/JAMC-D-14-0321.1>.
- Sen, P. K., 1968: Estimates of the regression coefficient based on Kendall's Tau. *J. Amer. Stat. Assoc.*, **63**, 1379–1389, <https://doi.org/10.1080/01621459.1968.10480934>.
- Sheffield, J., E. F. Wood, and M. L. Roderick, 2012: Little change in global drought over the past 60 years. *Nature*, **491**, 435–438, <https://doi.org/10.1038/nature11575>.
- Singh, D., D. L. Swain, J. Mankin, D. Horton, L. Thomas, B. Rajaratnam, and N. S. Diffenbaugh, 2016: Recent amplification of the North American winter temperature dipole. *J. Geophys. Res. Atmos.*, **121**, 9911–9928, <https://doi.org/10.1002/2016JD025116>.
- Slater, A. G., 2016: Surface solar radiation in North America: A comparison of observations, reanalyses, satellite, and derived products. *J. Hydrometeorol.*, **17**, 401–420, <https://doi.org/10.1175/JHM-D-15-0087.1>.
- Szilagyi, J., G. G. Katul, and M. B. Parlange, 2001: Evapotranspiration intensifies over the conterminous United States. *J. Water Resour. Plann. Manage.*, **127**, 354–362, [https://doi.org/10.1061/\(ASCE\)0733-9496\(2001\)127:6\(354\)](https://doi.org/10.1061/(ASCE)0733-9496(2001)127:6(354)).
- Udall, B., and J. T. Overpeck, 2017: The twenty-first century Colorado River hot drought and implications for the future. *Water Resour. Res.*, **53**, 2404–2418, <https://doi.org/10.1002/2016WR019638>.
- Urraca, R., T. Huld, A. Gracia-Amillo, F. J. Martinez-de-Pison, F. Kaspar, and A. Sanz-Garcia, 2018: Evaluation of global horizontal irradiance estimates from ERA5 and COSMO-REA6 reanalyses using ground and satellite-based data. *Sol. Energy*, **164**, 339–354, <https://doi.org/10.1016/j.solener.2018.02.059>.
- Vautard, R., J. Cattiaux, P. Yiou, J. N. Thépaut, and P. Ciais, 2010: Northern Hemisphere atmospheric stilling partly attributed to an increase in surface roughness. *Nat. Geosci.*, **3**, 756–761, <https://doi.org/10.1038/ngeo979>.
- Vicente-Serrano, S. M., and Coauthors, 2018: Recent changes of relative humidity: Regional connections with land and ocean processes. *Earth Syst. Dyn.*, **9**, 915–937, <https://doi.org/10.5194/esd-9-915-2018>.
- , T. R. McVicar, D. G. Miralles, Y. Yang, and M. Tomas-Burguera, 2020: Unraveling the influence of atmospheric evaporative demand on drought and its response to climate change. *Wiley Interdiscip. Rev. Climate Change*, **11**, e632, <https://doi.org/10.1002/wcc.632>.
- Vose, R. S., S. Applequist, M. J. Menne, C. N. Williams, and P. Thorne, 2012: An intercomparison of temperature trends in the U.S. Historical Climatology Network and recent atmospheric reanalyses. *Geophys. Res. Lett.*, **39**, L10703, <https://doi.org/10.1029/2012GL051387>.
- Walter, M. T., D. S. Wilks, J. Y. Parlange, and R. L. Schneider, 2004: Increasing evapotranspiration from the conterminous United States. *J. Hydrometeorol.*, **5**, 405–408, [https://doi.org/10.1175/1525-7541\(2004\)005<0405:IEFTCU>2.0.CO;2](https://doi.org/10.1175/1525-7541(2004)005<0405:IEFTCU>2.0.CO;2).
- Wen, C., A. Kumar, and Y. Xue, 2019: Uncertainties in reanalysis surface wind stress and their relationship with observing systems. *Climate Dyn.*, **52**, 3061–3078, <https://doi.org/10.1007/s00382-018-4310-4>.
- Westerling, A. L., H. G. Hidalgo, D. R. Cayan, and T. W. Swetnam, 2006: Warming and earlier spring increase western U.S. forest wildfire activity. *Science*, **313**, 940–943, <https://doi.org/10.1126/science.1128834>.
- Williams, A. P., and Coauthors, 2013: Temperature as a potent driver of regional forest drought stress and tree mortality. *Nat. Climate Change*, **3**, 292–297, <https://doi.org/10.1038/nclimate1693>.
- , and Coauthors, 2014: Causes and implications of extreme atmospheric moisture demand during the record-breaking 2011 wildfire season in the southwestern United States. *J. Appl. Meteor. Climatol.*, **53**, 2671–2684, <https://doi.org/10.1175/JAMC-D-14-0053.1>.
- , and Coauthors, 2015: Correlations between components of the water balance and burned area reveal new insights for predicting forest fire area in the southwest United States. *Int. J. Wildland Fire*, **24**, 14–26, <https://doi.org/10.1071/WF14023>.
- , and Coauthors, 2020: Large contribution from anthropogenic warming to an emerging North American megadrought. *Science*, **368**, 314–318, <https://doi.org/10.1126/science.aaz9600>.
- Woodhouse, C. A., G. T. Pederson, K. Morino, S. A. McAfee, and G. J. McCabe, 2016: Increasing influence of air temperature on Upper Colorado River streamflow. *Geophys. Res. Lett.*, **43**, 2174–2181, <https://doi.org/10.1002/2015GL067613>.
- Xia, Y., and Coauthors, 2009: NLDAS Primary Forcing Data L4 Hourly 0.125 × 0.125 degree V002 (NLDAS_FORA0125_H). GES DISC, accessed 1 January 2021, https://disc.gsfc.nasa.gov/datasets/NLDAS_FORA0125_H_002/summary.
- , and Coauthors, 2012: Continental-scale water and energy flux analysis and validation for the North American Land Data Assimilation System project phase 2 (NLDAS-2): 1. Intercomparison and application of model products. *J. Geophys. Res.*, **117**, D03109, <https://doi.org/10.1029/2011JD016048>.
- Yang, Y., M. L. Roderick, S. Zhang, T. R. McVicar, and R. J. Donohue, 2019: Hydrologic implications of vegetation response to elevated CO₂ in climate projections. *Nat. Climate Change*, **9**, 44–48, <https://doi.org/10.1038/s41558-018-0361-0>.
- Zeng, Z., and Coauthors, 2019: A reversal in global terrestrial stilling and its implications for wind energy production. *Nat. Climate Change*, **9**, 979–985, <https://doi.org/10.1038/s41558-019-0622-6>.
- Zhang, Z., K. Wang, D. Chen, J. Li, and R. Dickinson, 2019: Increase in surface friction dominates the observed surface wind speed decline during 1973–2014 in the northern hemisphere lands. *J. Climate*, **32**, 7421–7435, <https://doi.org/10.1175/JCLI-D-18-0691.1>.